

Supporting Information

A Novel Manganese Dioxide-Based Drug Delivery Strategy via In Situ Coating γ -Polyglutamic Acid/Cisplatin for Intelligent Anticancer Therapy

Zheng Zhang,^a Weichen Yan,^a Yuanhui Ji^{a}*

^aJiangsu Province Hi-Tech Key Laboratory for Biomedical Research, School of Chemistry and Chemical Engineering, Southeast University, Nanjing, 211189, China

***Correspondence: Prof. Dr. Yuanhui Ji**

No.2 Southeast University Road, Nanjing, Jiangsu 211189, China

E-mail: yuanhui.ji@seu.edu.cn; yuanhuijinj@163.com

Supplementary Figures and Tables:

Fig. S1. TEM-energy dispersive X-ray spectroscopy (EDS) of the PGA/CDDP@MnO₂ NPs.

Fig. S2. FESEM-EDS of the PGA/CDDP@MnO₂ NPs.

Fig. S3. Wide-scan X-ray photoelectron spectroscopy (XPS) spectra (a), C1s (b), O1s (c), and Pt4f (d) spectra of PGA/CDDP@MnO₂ NPs.

Fig. S4. X-ray diffraction (XRD) of PGA/CDDP@MnO₂ NPs.

Table S1. Parameters k , n and R^2 determined by Eq. (1) for the CDDP release of PGA/CDDP@MnO₂ NPs at different release conditions.

Fig. S5. Plots of $\ln(M_t/M_\infty)$ versus $\ln t$ for the release profiles of PGA/CDDP@MnO₂ NPs under different GSH conditions.

Fig. S6. Plots of $\ln(M_t/M_\infty)$ versus $\ln t$ for the release profiles of PGA/CDDP@MnO₂ NPs under different PBS conditions.

Fig. S7. HR-TEM images of the PGA/CDDP@MnO₂ NPs after degradation (24 h) in GSH and PBS medium.

Fig. S8. High magnification image of PGA/CDDP@MnO₂ NPs after degradation in GSH medium (10 mM) for 24 h (a: scale bar = 50 nm, b: scale bar = 20 nm).

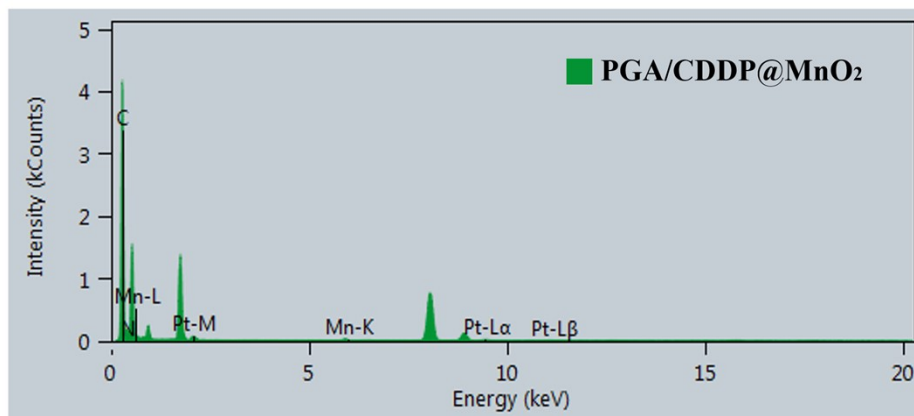


Fig. S1. TEM-energy dispersive X-ray spectroscopy (EDS) of PGA/CDDP@MnO₂ NPs.

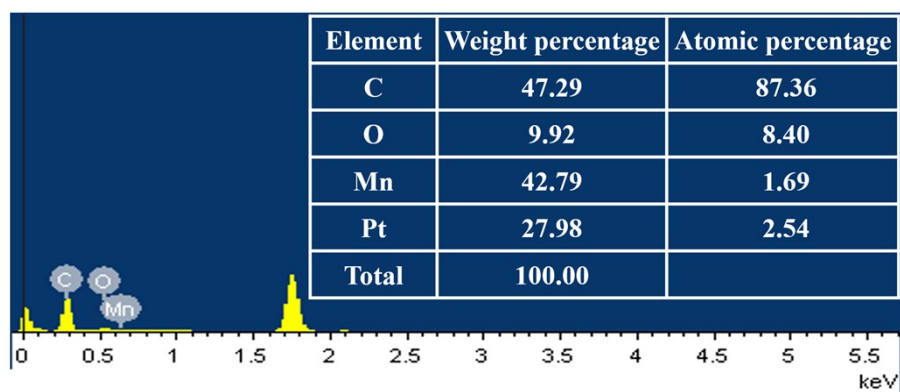


Fig. S2. FESEM-energy dispersive X-ray spectroscopy (EDS) of PGA/CDDP@MnO₂ NPs..

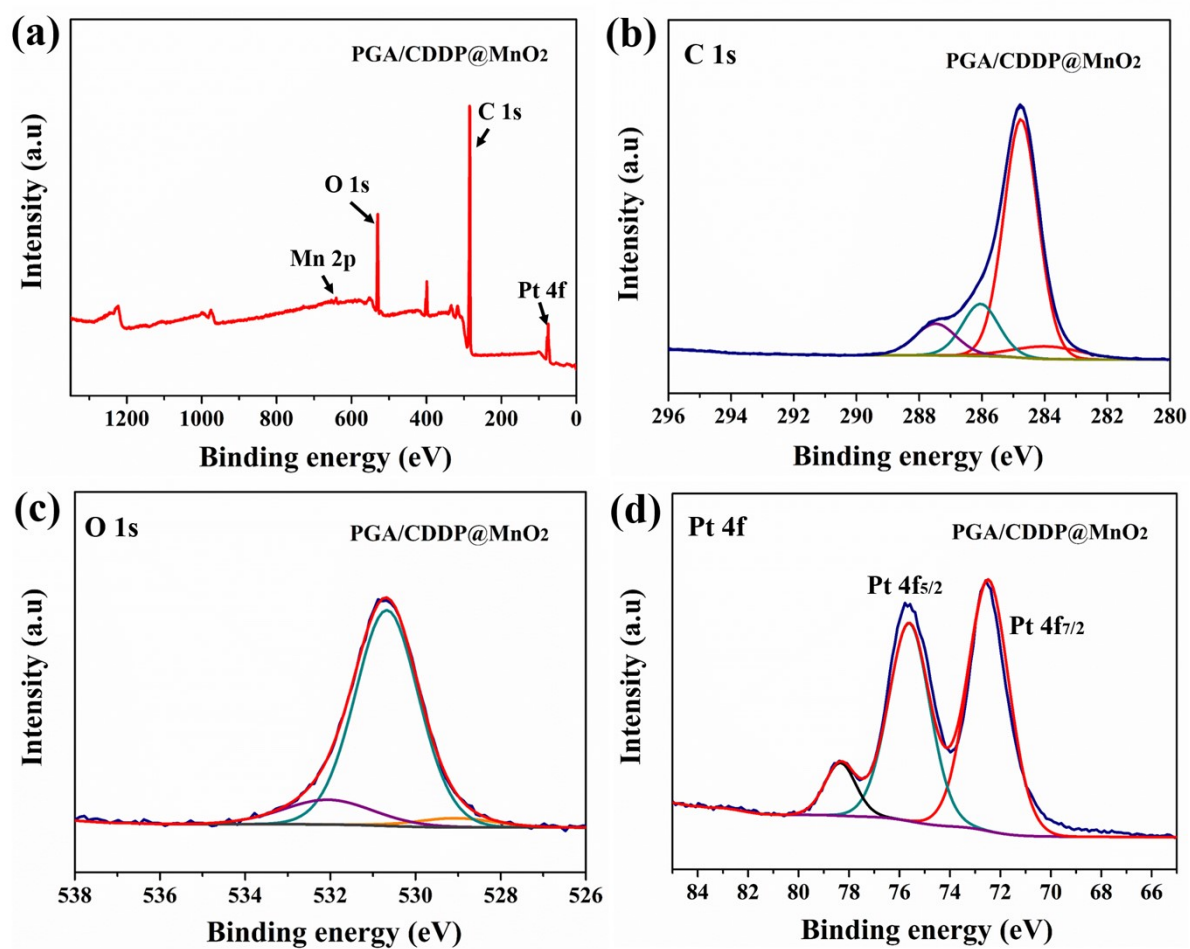


Fig. S3. The wide-scan X-ray photoelectron spectroscopy (XPS) spectra (a), C1s (b), O1s (c), and Pt4f (d) spectra of PGA/CDDP@MnO₂ NPs.

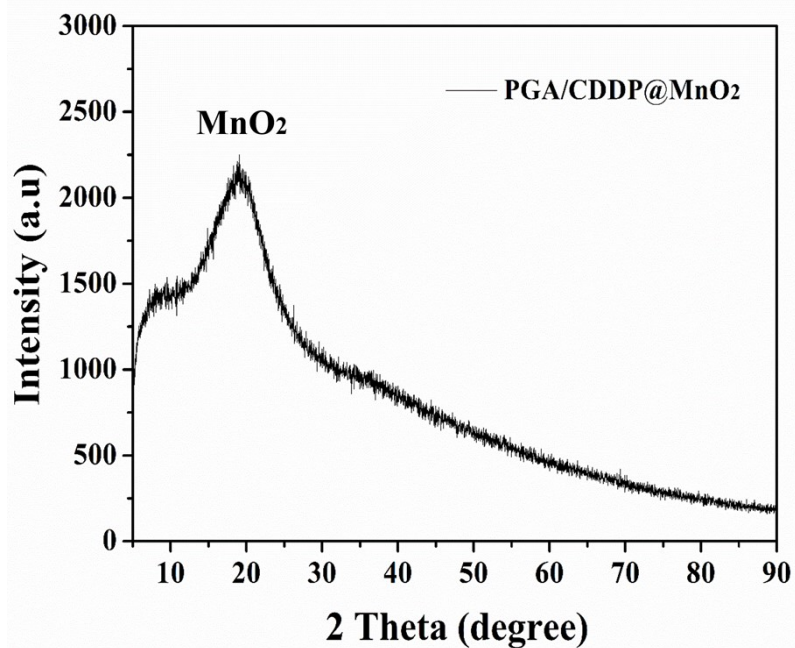


Fig. S4. X-ray diffraction (XRD) spectrum of PGA/CDDP@MnO₂ NPs.

Table S1. Parameters k , n and R^2 determined by Eq. (1) for the CDDP release from PGA/CDDP@MnO₂ NPs at different release conditions.

Sample	Release condition	k	n	R^2
PGA/CDDP@MnO ₂ NPs	GSH=2 mM	3.63×10^{-7}	0.9703	0.9134
PGA/CDDP@MnO ₂ NPs	GSH=5 mM	8.06×10^{-7}	1.0077	0.9653
PGA/CDDP@MnO ₂ NPs	GSH=10 mM	8.24×10^{-7}	0.9338	0.6811
PGA/CDDP@MnO ₂ NPs	pH 6.5	7.31×10^{-5}	0.5827	0.9908
PGA/CDDP@MnO ₂ NPs	pH 4.5	1.10×10^{-8}	1.5131	0.8020
PGA/CDDP@MnO ₂ NPs	pH 2.1	4.64×10^{-6}	0.1376	0.9428

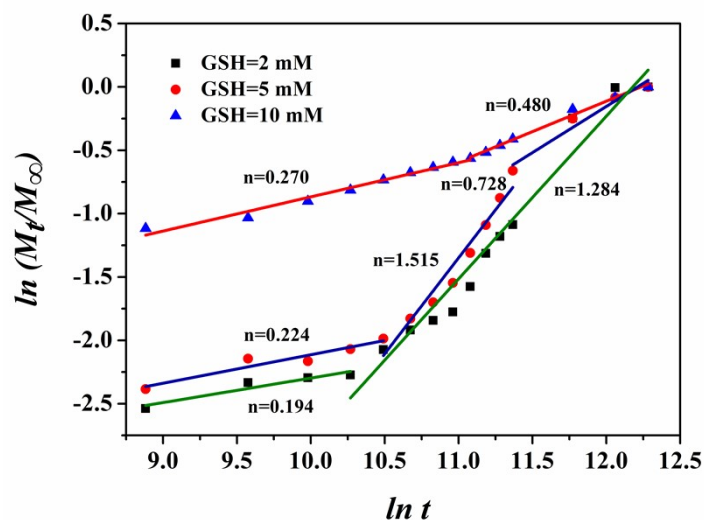


Fig. S5. Plots of $\ln(M_t/M_\infty)$ versus $\ln t$ for the release profiles of PGA/CDDP@MnO₂ NPs under different GSH conditions.

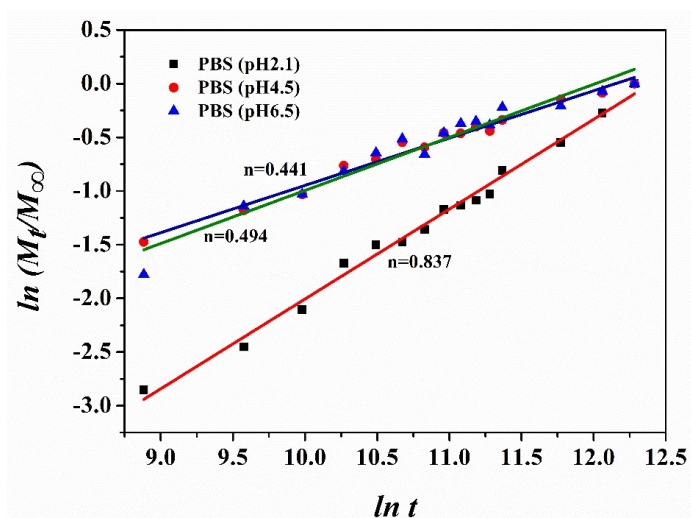


Fig. S6. Plots of $\ln(M_t/M_\infty)$ versus $\ln t$ for the release profiles of PGA/CDDP@MnO₂ NPs under different PBS conditions.

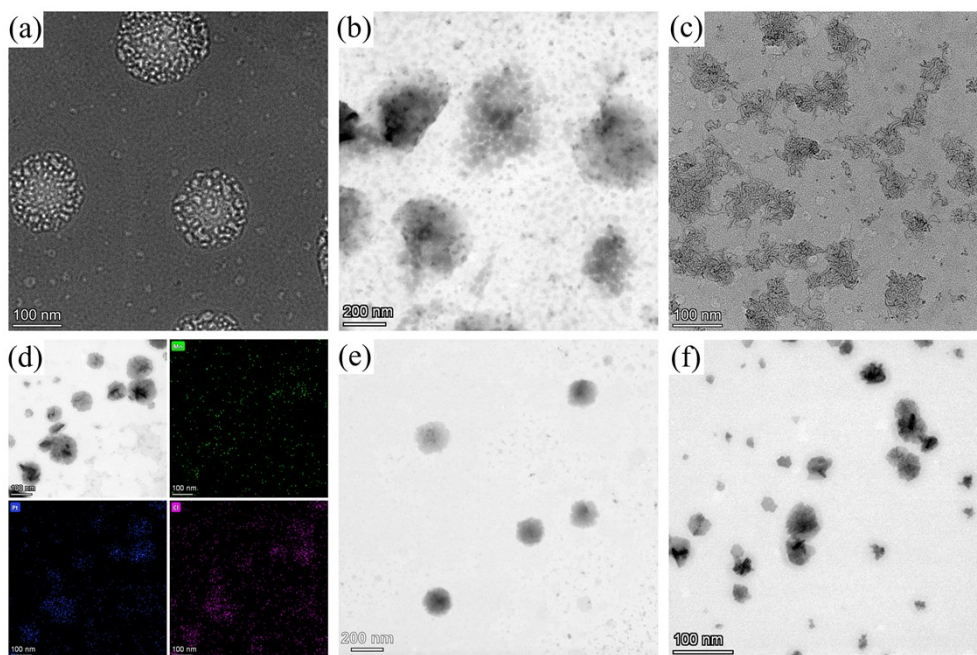


Fig. S7. HR-TEM images of the PGA/CDDP@MnO₂ NPs after degradation (24 h) in GSH medium with the concentration of 2 mM (a), 5 mM (b), and 10 mM (c). HR-TEM image and elemental mapping of PGA/CDDP@MnO₂ NPs after degradation in PBS medium with pH 6.5 (d), pH 4.5 (e), and pH 2.1 (f).

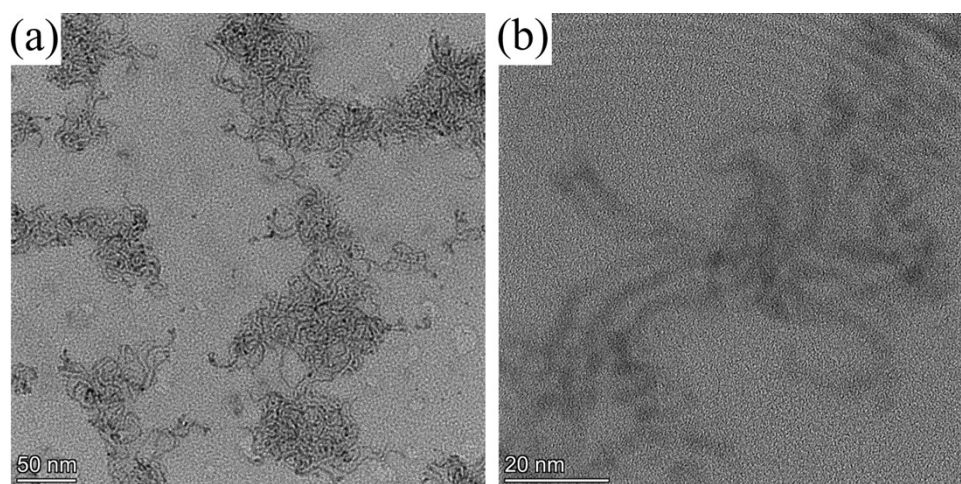


Fig. S8. The high magnification image of PGA/CDDP@MnO₂ NPs after degradation in GSH medium (10 mM) for 24 h (a: scale bar = 50 nm, b: scale bar = 20 nm).